Bone Reports 5 (2016) 1–6

Contents lists available at ScienceDirect

Bone Reports

journal homepage: www.elsevier.com/locate/bonr

Cdc42 is crucial for facial and palatal formation during craniofacial development

Mutsuko Oshima-Nakayama [a,b,1], Atsushi Yamada [a,*,1], Tamaki Kurosawa [a], Ryo Aizawa [a,c], Dai Suzuki [a], Yoshiro Saito [a,d], Hidetoshi Kassai [e], Yuki Sato [b], Matsuo Yamamoto [c], Tatsuo Shirota [d], Atsu Aiba [e], Koutaro Maki [b], Ryutaro Kamijo [a]

[a] Department of Biochemistry, School of Dentistry, Showa University, Shinagawa, Tokyo 142-8555, Japan.
[b] Department of Orthodontics, School of Dentistry, Showa University, Ohta, Tokyo 145-8515, Japan
[c] Department of Periodontology, School of Dentistry, Showa University, Ohta, Tokyo 145-8515, Japan
[d] Department of Oral and Maxillofacial Surgery, School of Dentistry, Showa University, Ohta, Tokyo 145-8515, Japan
[e] Laboratory of Animal Resources, Center for Disease Biology and Integrative Medicine, Faculty of Medicine, The University of Tokyo, Bunkyo-ku, Tokyo 113-0033, Japan

ARTICLE INFO

Article history:
Received 22 June 2015
Received in revised form 15 December 2015
Accepted 4 January 2016
Available online 8 January 2016

Keywords:
Cdc42
Cleft palate
Conditional knockout mice
P0-cre transgenic mice

ABSTRACT

Craniofacial deformities with multifactorial etiologies, such as cleft palate and facial dysmorphism, represent some of the most frequent congenital birth defects seen in humans. Their pathogeneses are often related to cranial neural crest (CNC) cells. During CNC cell migration, changes in cell shape and formation, as well as maintenance of subcellular structures, such as filopodia and lamellipodia, are dependent on the complex functions of Rho family small GTPases, which are regulators of actin cytoskeletal organization. Cdc42, a member of the Rho family of small GTPases, is known to play critical roles in organogenesis of various tissues. To investigate the physiological functions of Cdc42 during craniofacial development, we generated CNC-derived cell-specific inactivated Cdc42 mutant mice (*Cdc42*$^{fl/fl}$;*P0-cre*). Most of the *Cdc42*$^{fl/fl}$;*P0-cre* neonates were viable at birth, though they appeared weaker and no milk was found in their stomachs, and all died within a few days. They had a short face and intracranial bleeding, and abnormal calcification of the cranium. *Cdc42*$^{fl/fl}$;*P0-cre* neonates also demonstrated a cleft palate and there was no fusion of the secondary palate because of failure of palatal shelf elongation for the process of palate closure. Cdc42 is crucial for facial and palatal formation during craniofacial development.

1. Introduction

Cleft lip with or without cleft palate occurs in 1 in 500 to 2500 live births worldwide, and represents the most frequent congenital facial anomaly seen in humans. The condition, which requires complex multidisciplinary treatments and has lifelong implications for affected individuals (Vanderas, 1987; Schutte and Murray, 1999), is caused by various pathogenetic influences, such as genetics and environmental risk factors, as well as others (Wilkie and Morriss-Kay, 2001; Cobourne, 2004). Cleft lip and palate seen in affected humans are caused by abnormal facial development during fusion of the medial nasal process and maxillary process between 5 to 8 weeks after fertilization (Levi et al., 2011). The definitive mammalian palate forms through union of the primary palate and 2 secondary palatal shelves. Palatal development is the process in which the bilateral maxillary processes descend vertically from the maxilla, and occurs between embryonic day (E)12.5 and E15.5. Subsequently, the palatal shelves rotate horizontally, then meet at the midline and fuse by E15.5, followed by disappearance of the midline epithelial seam (Ferguson, 1977; Liu et al., 2007). One of the key features of craniofacial development is formation of neural crest (NC) cells (Le Douarin et al., 2004).

NC cells are embryonic multi-potent stem cells that give rise to various types of cells and tissues (Bronner-Fraser and Fraser, 1988; Shah et al., 1996). Among the various types, cranial neural crest (CNC) cells play important roles in the regulation of craniofacial development (Bronner-Fraser, 1993; Selleck et al., 1993), while it is also known that they form most of the hard tissues of the head, such as the maxilla, mandible, and teeth (Chai and Maxson, 2006). During CNC cell migration, changes in cell shape and formation, as well as maintenance of subcellular structures, such as filopodia and lamellipodia, are dependent on members of the Rho family of small G proteins. Cdc42, a Rho family small G protein, is ubiquitously expressed and functions as a molecular switch, cycling between an active and inactive GDP-bound states (Van Aelst and D'Souza-Schorey, 1997; Etienne-Manneville and Hall, 2002), while it is also known to play critical roles in cellular functions, such

* Corresponding author at: Department of Biochemistry, School of Dentistry, Showa University, 1-5-8 Hatanodai, Shinagawa, Tokyo 142-8555, Japan.
E-mail address: yamadaa@dent.showa-u.ac.jp (A. Yamada).
[1] These authors contributed equally to this work.

http://dx.doi.org/10.1016/j.bonr.2016.01.001

as actin cytoskeletal reorganization, cell migration, differentiation, and gene expression (Bishop and Hall, 2000; Jaffe and Hall, 2005). Cdc42 conventional knockout mice die before E7.5 (Chen et al., 2000). Using tissue-specific gene knockout technology, Cdc42 has been indicated to play various critical roles in vivo (Hall and Nobes, 2000; Liu et al., 2013).

Recently, Aizawa et al. (2012) demonstrated the functions of Cdc42 during limb development using limb bud mesenchyme-specific inactivated Cdc42 (*Cdc42*$^{fl/fl}$;*Prx1-cre*) mice. Those mice demonstrated a cleft palate because of failure of palatal shelf elongation (Aizawa et al., 2012). Liu et al. (2013) also reported that Cdc42 plays an essential role in NC cell migration, and inactivation of Cdc42 in NC cells impaired craniofacial and cardiovascular development in mice. To investigate the physiological functions of Cdc42 during facial and palatal development, we used a well-characterized transgene in which Cre-recombinase is driven by a promoter of protein 0 (P0), a specific marker of NC cells (Yamauchi et al., 1999). This transgene expresses Cre in tissues derived from NC cells, such as spinal dorsal root ganglia, the sympathetic and enteric nervous systems, and ventral craniofacial mesenchyme during stages later than E9.0.

2. Materials and methods

2.1. Generation of Cdc42 conditional knockout mice

All animal experiments were conducted in accordance with the guidelines of Showa University and the University of Tokyo. The *Cdc42 gene* was knocked out using Cre-loxP recombination by crossing *Cdc42* flox with *P0-cre* transgenic (*P0-cre*) mice (Yamauchi et al., 1999; Aizawa et al., 2012). Timed-mating was set to occur on noon of the day on which a vaginal plug was detected and was considered to be E0.5. Offspring were genotyped by PCR analysis using the following primer pairs: for *P0-Cre*, 5′-GACGATGCAACGAGTGATGA-3′ and 5′-AGCA TTGCTGTCACTTGGTC-3′; and for *Cdc42*, F1 5′-ATCGGTCACTGTTCTACT TTG-3′ and R1 5′-TACTGCTATGACTGAAAACCTC-3′. Both conditional and Δexon2 alleles were identified using F1, R1, and R2 5′-GTTTT GCCTGCATGTATGTCTG-3′ primers (Fig. 1A).

For analyses of expression patterns generated by *P0*-mediated Cre recombination, R26R reporter mice and CAG-CAT-EGFP transgenic mice were used (Soriano, 1999; Kawamoto et al., 2000). R26R reporter mice carry a *loxP-stop-loxP-lacZ* cassette inserted into the ubiquitously expressed ROSA26 locus. Mating of *P0-cre* with *R26R* reporter mice generated double transgenic mice (*R26R*;*P0-cre* mice), then detection of β-galactosidase activity in whole embryos was performed as previously described (Chai et al., 2000). Also, mating of *P0-cre* mice with CAG-CAT-EGFP transgenic mice generated double transgenic mice (*EGFP*;*P0-cre* mice), with detection of EGFP in the palate of E13.5 mice examined using fluorescence stereomicroscopy (MVX100, OLYMPUS). The genetic background of the mice used in this study is a hybrid of the C57BL/6, 129Ola, and ICR strains.

2.2. Quantitative real-time PCR

Total RNA from palates was extracted with TRIzol reagent (Life Technologies), then reverse transcribed using SuperScript III (Life Technologies). Quantitative PCR was performed using a TaqMan real-time PCR system, with the following assay IDs: Cdc42; Mm01194005g1, *CyclinD*$_1$; Mm00432359m1, and *Gapdh*; Mm03302249g1.

2.3. Anatomical and histological analyses

For skeletal staining, mice were skinned and eviscerated, then dehydrated in 95% ethanol overnight. The skeletons were stained

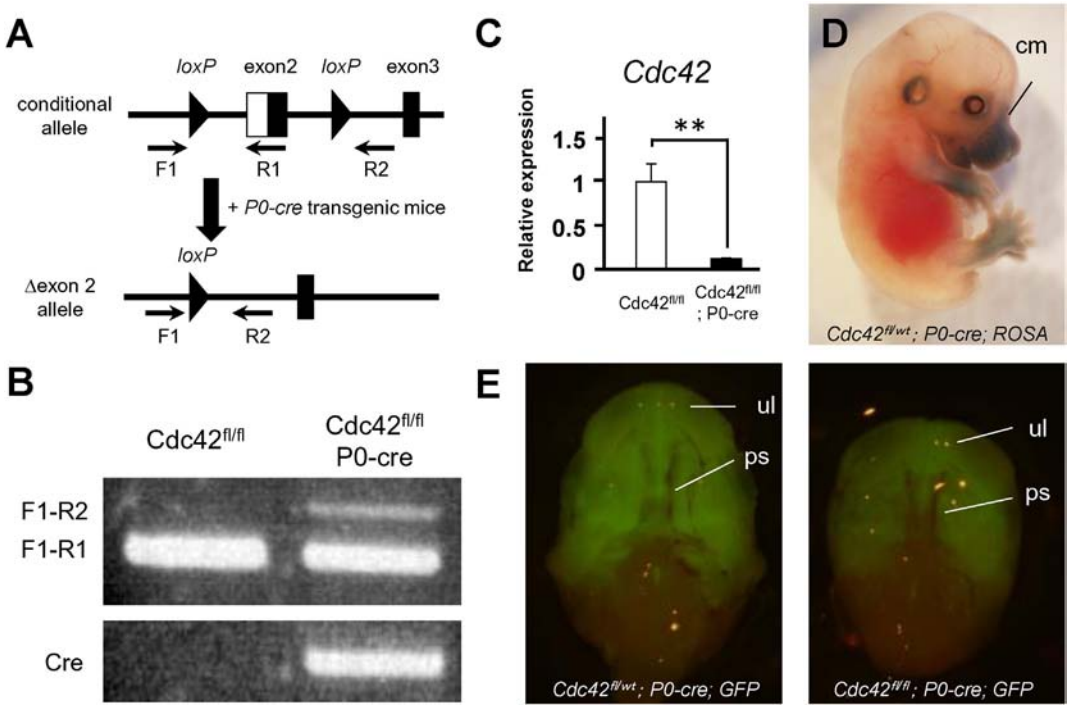

Fig. 1. Generation of *Cdc42* conditional knockout mice. (A) Schematic drawing of targeted strategy for production of *Cdc42* conditional knockout mice. Different primers (F1, R1, R2) were used for PCR assessment of *Cdc42* exon 2 deletion (Δexon2). (B) PCR was performed using *Cdc42*$^{fl/fl}$ and *Cdc42*$^{fl/fl}$;*P0-cre* palate samples obtained on postnatal day 0. Conditional allele specific (F1–R1; 162 bp) and Δexon 2 allele specific (F1–R2; 350 bp) gene expressions were found. (C) The expression level of *Cdc42* was determined using real-time PCR. Amplification signals from the *Cdc42* gene were normalized against those from the *Gapdh* gene. Values are shown as the mean ± SD of 3 samples as compared to the level seen with *Cdc42*$^{fl/fl}$ (**P < 0.01). (D) Detection of β-galactosidase (*lacZ*) activity. Temporal and spatial expressions of *lacZ* in whole-mount X-gal-stained embryos of *Cdc42*$^{fl/wt}$;*P0-cre*;*R26R* mice on E13.5. Lateral views demonstrated that β-galactosidase activity was mostly observed in the area of neural crest migration. cm; cranial mesenchyme. (E) Localization of NC-derived cells in palates of *Cdc42*$^{fl/wt}$;*P0-cre*;*EGFP* and *Cdc42*$^{fl/fl}$;*P0-cre*;*EGFP* mice on E13.5. Stereoscopic fluorescence microscope images of palates. Panels show corresponding fluorescent images. GFP labeled cells (green) were observed in the palates. ul; upper lip, ps; palatal shelf. (For interpretation of the references to color in this figure legend, the reader is referred to the web version of this article.)

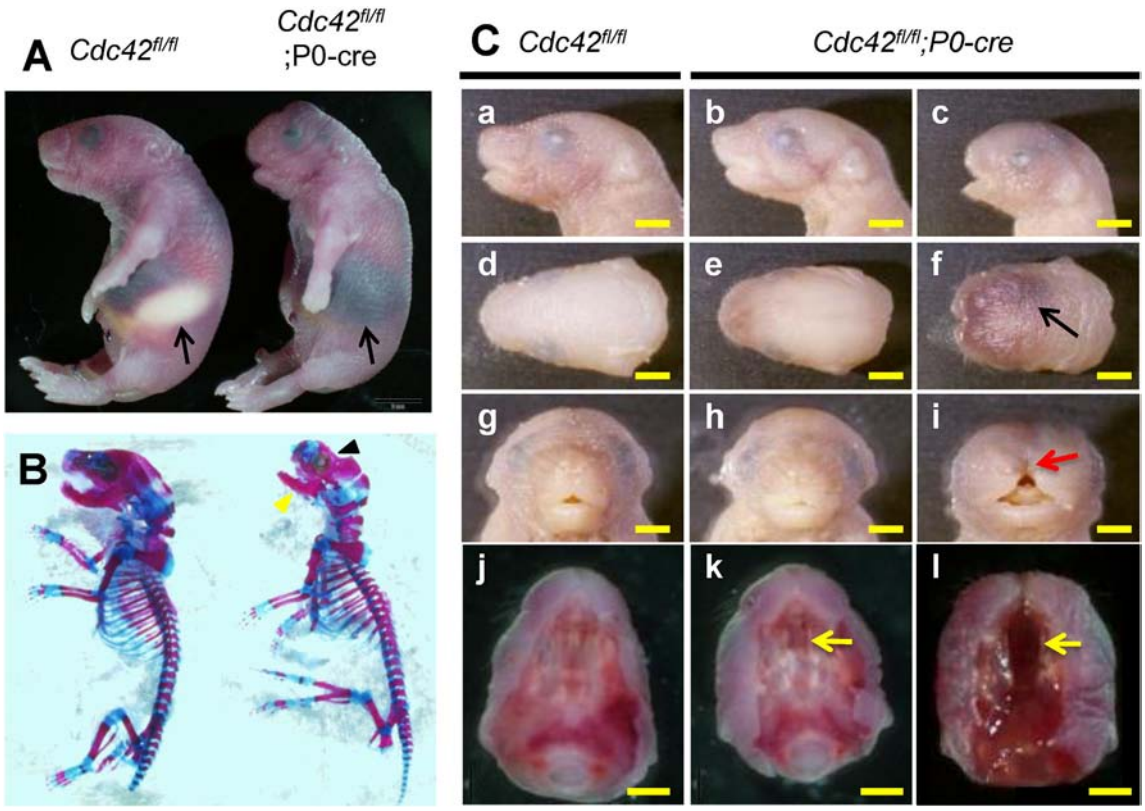

Fig. 2. Craniofacial defects in *Cdc42* conditional knockout mice. (A) Lateral view on postnatal day 0. No milk was observed in the stomachs of *Cdc42*$^{fl/fl}$;*P0-cre* mice (black arrows). (B) Skeletal staining with alcian blue and alizarin red on postnatal day 0. Severe deformities were observed in the frontal (black arrowhead) and mandible (yellow arrowhead) bones of *Cdc42*$^{fl/fl}$;*P0-cre* mice. (C) Lateral (a–c), dorsal (d–f), frontal (g–i), and oral (j–l) views obtained on postnatal day 0. Intracranial bleeding (f, black arrow), cleft face (i, red arrow), and cleft palate (k and l, yellow arrows) were observed in *Cdc42*$^{fl/fl}$;*P0-cre* mice. Scale bar = 1 mm. (For interpretation of the references to color in this figure legend, the reader is referred to the web version of this article.)

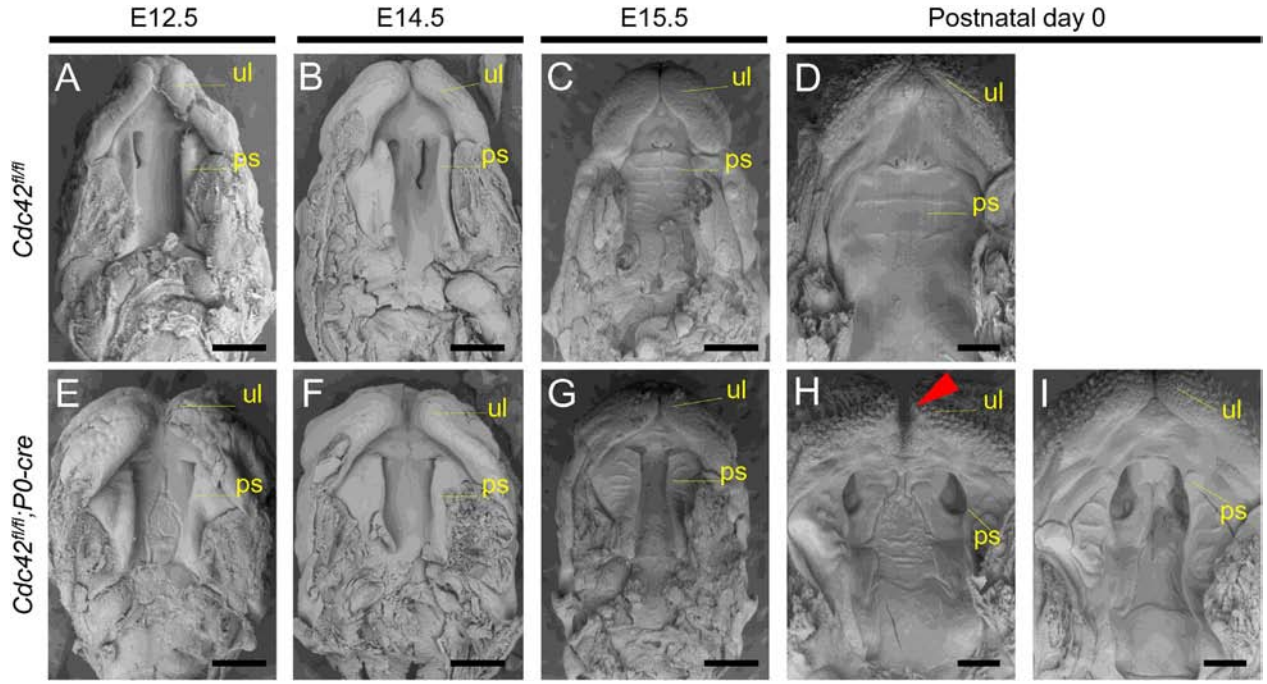

Fig. 3. Scanning electron microscopy analysis of palatal defects in Cdc42 conditional knockout mice. Oral view of developing palates of *Cdc42*$^{fl/fl}$ and *Cdc42*$^{fl/fl}$;*P0-cre* mice from E12.5 to postnatal day 0. The lower jaw was removed for a better view of the palate. Coalescence of the palatal shelf was observed in *Cdc42*$^{fl/fl}$ but not *Cdc42*$^{fl/fl}$;*P0-cre* mice on E15.5 (C, G). ul; upper lip, ps; palatal shelf. Scale bar = 500 μm.

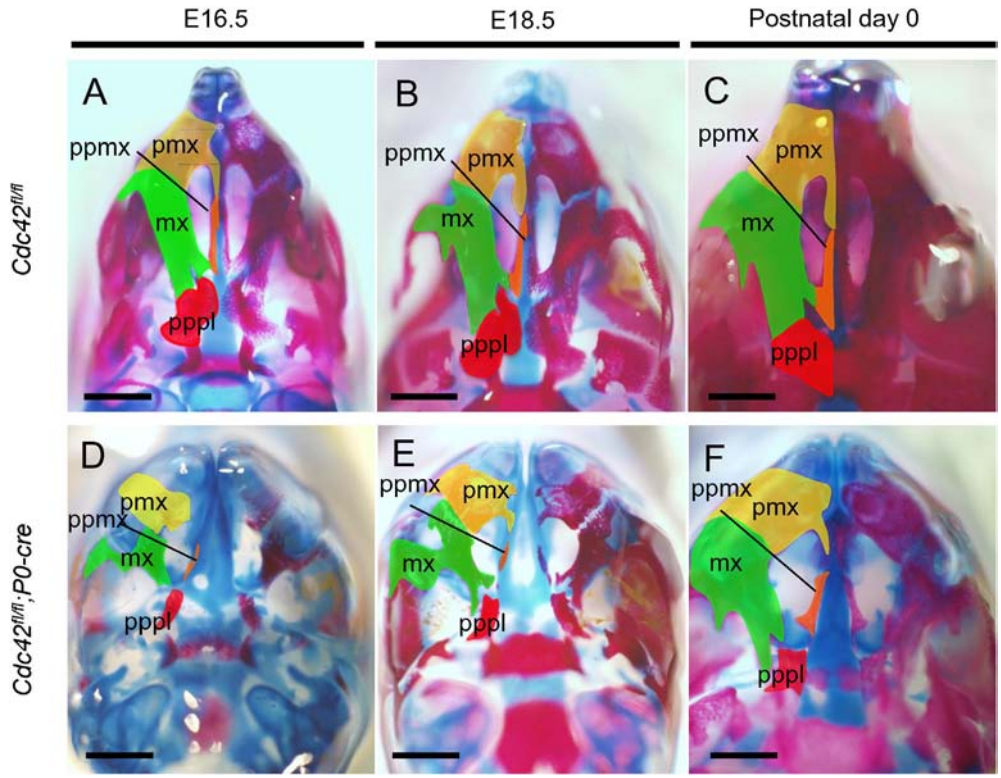

Fig. 4. Craniofacial skeleton defects in Cdc42 conditional knockout mice. The developing mandible and tongue were removed. Maxilla preparations were stained with alcian blue and alizarin red. The oral view of the maxilla showed dysplasia in the frontal bones including the maxilla (green region) and premaxilla (yellow region) areas. The palatal processes of the maxilla (orange region) and palatine (pink region) showed hypoplasia. pmx; premaxilla, ppmx; palatal process of maxilla, pppl; palatal process of palatine, premaxilla length; black bar, maxilla length; yellow bar. Scale bar = 2 mm. (For interpretation of the references to color in this figure legend, the reader is referred to the web version of this article.)

overnight with 0.015% alcian blue and 10% acetic acid in 75% ethanol, and soft tissues were dissolved overnight in 2% KOH, while the skeletons were additionally stained overnight with 0.0075% alizarin red in 1% KOH. Finally, the skeletons were cleared in 0.5% KOH and 20% glycerol for several days, and stored in glycerol/ethanol (1:1). For general morphological examinations, all samples were fixed in 4% paraformaldehyde (PFA) and processed into serial paraffin sections using routine procedures. Deparaffinized coronal sections (4 μm thick) were serially prepared from the anterior to posterior of the palate and stained with hematoxylin and eosin (HE).

For scanning electron microscopy (SEM) analyses, all samples were fixed in 4% PFA, 2.5% glutaraldehyde, and osmic acid. After dehydration through a graded ethanol series, samples were critical-point dried in a Blazer dryer, ion-sputtered with platinum–palladium (80 nm), and observed with a TM3000 microscope (HITACHI).

2.4. Statistical analysis

All values are expressed as the mean ± SD. Statistical analysis was performed using a two-tailed Student's t test. P values < 0.05 were considered to be statistically significant.

3. Results

3.1. Generation of Cdc42 conditional knockout mice using CNC derived cells

To investigate the role of *Cdc42* in craniofacial and palatal development, we studied the effect of inactivating *Cdc42* by the use of a Cre-loxP system for CNC-derived cell-specific inactivation of the *Cdc42* gene in *P0-cre* mice, since *Cdc42* conventional knockout mice (*Cdc42*$^{-/-}$) show embryonic lethality and die before E7.5 (Chen et al., 2000). To verify recombination of the *Cdc42* conditional allele by Cre leading to the Δexon 2 allele of the *Cdc42* gene, we used PCR assays with genomic DNA and RNA isolated from palates on postnatal day 0 (Fig. 1B, C). To investigate the ability of the *P0* gene promoter driving the Cre recombinase transgene, *P0-cre* mice were bred with targeted gene trap ROSA26 reporter mice (R26R). Cre-mediated recombination in R26R mice induces LacZ expression, which can be monitored by LacZ staining. LacZ staining was detected in cranial mesenchyme on E13.5 (Fig. 1D). To confirm localization of CNC-derived cells in the palate, we also analyzed *EGFP-P0-cre* mice. CNC-derived cells were identified by evaluating GFP expression after *P0-cre*-mediated DNA recombination (Fig. 1E).

3.2. Cdc42 conditional mutant mice show severe craniofacial and palatal defects

Cdc42$^{fl/fl}$;*P0-cre* mice were present in a Mendelian ratio up to birth (*Cdc42*$^{fl/wt}$;*P0-cre*: n = 16/55, *Cdc42*$^{fl/fl}$;*P0-cre*: n = 15/55, *Cdc42*$^{fl/wt}$: n = 11/55, *Cdc42*$^{fl/fl}$: n = 13/55) and nearly all *Cdc42*$^{fl/fl}$;*P0-cre* mice died within 1 day after birth. *Cdc42*$^{fl/fl}$;*P0-cre* neonates appeared weaker as compared to their *Cdc42*$^{fl/fl}$ littermates and no milk was found in their stomachs (Fig. 2A). In *Cdc42*$^{fl/fl}$;*P0-cre* mice, severe deformities were observed in the cranial bones, especially frontal, nasal, premaxilla, and mandible bone specimens (Fig. 2B). *Cdc42*$^{fl/fl}$;*P0-cre* mice also showed short snouts (n = 13/15) (Fig. 2C b, c), while this phenotype was not present in *Cdc42*$^{fl/fl}$ mice (Fig. 2C a). The most striking feature of *Cdc42*$^{fl/fl}$;*P0-cre* mice was cleft palate (n = 15/15) (Fig. 2C k, l). Most *Cdc42*$^{fl/fl}$;*P0-cre* mice exhibited both a cleft face and cleft palate (n = 13/15) (Fig. 2C i, l), while the 2 that did not exhibited only a cleft palate (n = 2/15) (Fig. 2C h, k). We also occasionally observed intracranial bleeding in *Cdc42*$^{fl/fl}$;*P0-cre* mice (Fig. 2C f).

In addition to the palate developmental defects shown in Fig. 2C, scanning electron microscopy (SEM) examinations were performed between E12.5 and postnatal day 0. In mice, palatal shelves grow downward from the maxillary processes, lateral to the tongue on E12.5,

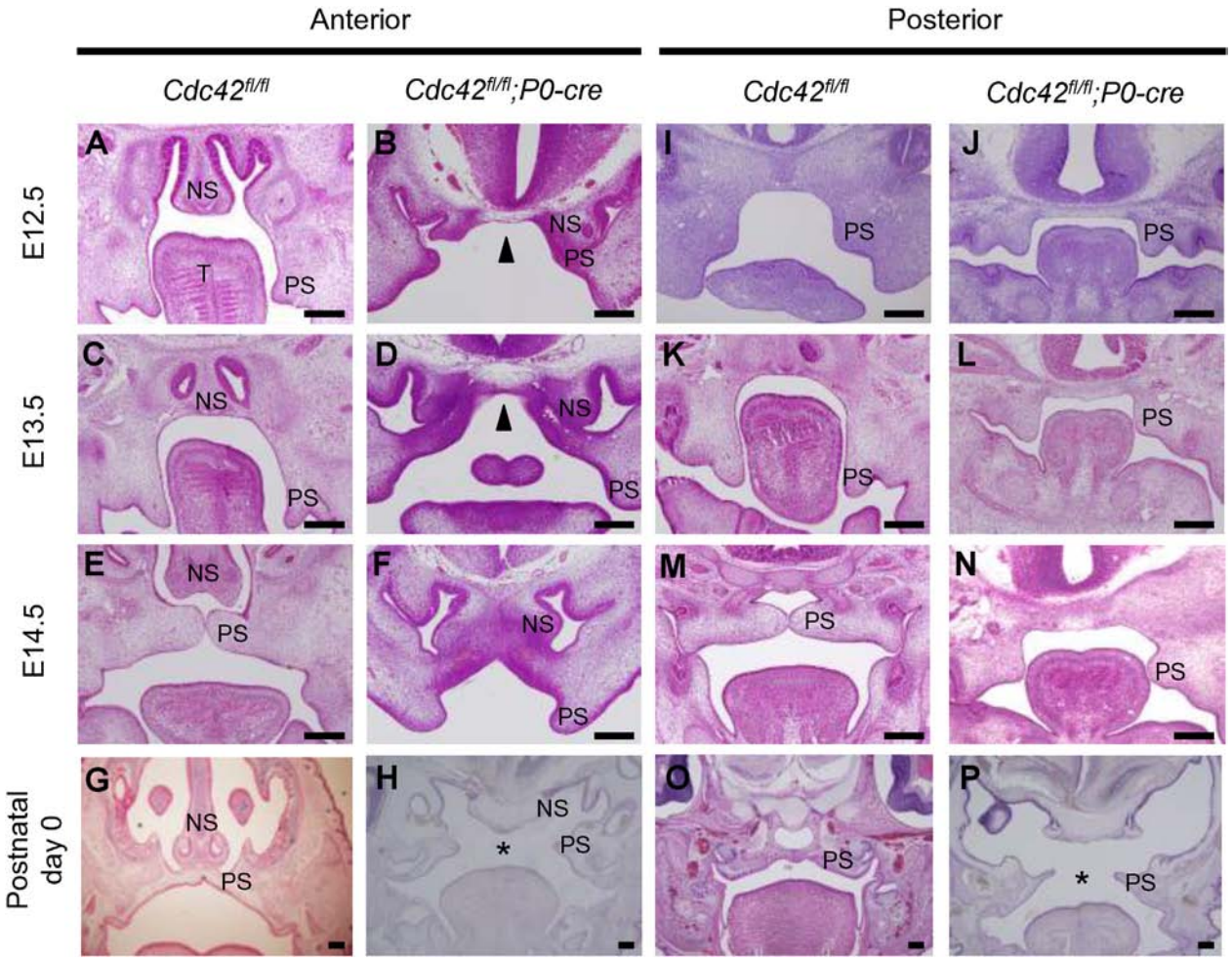

Fig. 5. Histological analysis of developing palates in Cdc42 conditional knockout mice. Hematoxylin and eosin staining of coronal sections of palates on E12.5 and postnatal day 0. The medial nasal processes failed to merge and the nasal septum was divided in *Cdc42*$^{fl/fl}$;*P0-cre* mice (B and D, black arrows), and the palatal shelves remained separated (H and P, black asterisk). T; tongue, PS; palatal shelf, NS; nasal septum. Scale bar = 200 μm.

then rotate and become elevated above the tongue by E13.5, extend towards the midline on E14.5, and become fused by E15.5 (Liu et al., 2007). The morphological structures of the palatal shelves in *Cdc42*$^{fl/fl}$;*P0-cre* mice were comparable with those in *Cdc42*$^{fl/fl}$ mice up to E14.5 (Fig. 3A, B, E, F). However, a pronounced aberration in palate development was observed in the *Cdc42*$^{fl/fl}$;*P0-cre* mice on E15.5, by which time the *Cdc42*$^{fl/fl}$ mice palate shelves had begun to fuse at the midline (Fig. 3C, G). All *Cdc42*$^{fl/fl}$;*P0-cre* mice exhibited a cleft palate (Fig. 3H, I).

We next examined cranial skeletons of *Cdc42*$^{fl/fl}$;*P0-cre* mice. Skeletal preparations of the upper jaw were stained with alcian blue, which stains all cartilaginous elements, and alizarin red, which stains mineralized bone matrix (Fig. 4). We observed significant frontal bone dysplasia (either reduced ossification or hypoplasia) in *Cdc42*$^{fl/fl}$;*P0-cre* mice as compared with *Cdc42*$^{fl/fl}$ mice on E16.5 and E18.5 (Fig. 4A, B, D, E), while an unfused nasal capsule premaxilla was observed in *Cdc42*$^{fl/fl}$;*P0-cre* mice. The lengths of the premaxilla (mean = 2.37 ± 0.32 vs. 1.78 ± 0.20 mm; n = 4; $P < 0.05$) and maxilla (mean = 5.67 ± 0.10 vs. 4.40 ± 0.11 mm; n = 4; $P < 0.05$) bones were shorter in *Cdc42*$^{fl/fl}$;*P0-cre* mice as compared with *Cdc42*$^{fl/fl}$ mice on postnatal day 0, which caused a reduction in snout length (Fig. 4C, F). We also observed that the palatal processes of the maxilla and palatine showed hypoplasia in *Cdc42*$^{fl/fl}$;*P0-cre* mice as compared with *Cdc42*$^{fl/fl}$ mice on E16.5 and E18.5 (Fig. 4A, B, D, E). As a result, palatal shelves associated with hypoplastic palatine bone were absent in *Cdc42*$^{fl/fl}$;*P0-cre* mice (Fig. 4C, F).

To perform histological analyses of palatal development, we examined 2 positions along the antero-posterior axis of the palate from E12.5 to postnatal day 0. On E12.5 and 13.5, failure of merging the medial nasal processes was observed in *Cdc42*$^{fl/fl}$;*P0-cre* mice, and the nasal septum was divided into right and left in the anterior position (Fig. 5B, F). In addition, *Cdc42*$^{fl/fl}$;*P0-cre* mice exhibited palatal shelf elevation failure and their palatal shelves remained separate from each other (Fig. 5B, D, F, H in anterior position, J, L, N, P in posterior position).

4. Discussion

In the present study, we investigated phenotypes of Cdc42 conditional knockout mice by deleting the *Cdc42* gene in CNC-derived cells from *P0-cre* transgenic mice. Previously, *Cdc42*$^{fl/fl}$;*Prx1-cre* mice, which lack the *Cdc42* gene in limb buds and cranial mesenchyme, were found to have a cleft palate and reduced ossification of the cranium, including the frontal and parietal bones, as well as intracranial bleeding, which was likely caused by retarded fusion between the parietal and occipital bones (Aizawa et al., 2012). Interestingly, in another study, *Rac1*$^{fl/fl}$;*Prx1-cre* mice also demonstrated a hypoplastic cranium, including the parietal and occipital bones, and intracranial bleeding, but not a cleft palate (Suzuki et al., 2009). It should be noted that Fuchs et al. reported that NC-derived cell-specific inactivation of the *Cdc42* gene using *Wnt1-cre* (*Cdc42*$^{fl/fl}$;*Wnt1-cre* mice) caused death before E14.5 and the mice showed craniofacial abnormalities, including a facial cleft (Fuchs et al., 2009).

In *Cdc42*$^{fl/fl}$;*Wnt1-cre* mice, cell proliferation is insufficient for NC target tissue formation due to premature exit from the cell cycle

(Fuchs et al., 2009). Liu et al. (2013) also noted that *Cdc42*$^{fl/fl}$;*Wnt1-cre* mice, whose genetic background is different from those in the study of Fuchs, survived up to E18.5 and had craniofacial defects along with a short snout, encephalocele formation, and a cleft lip and palate. The phenotypes of the *Cdc42*$^{fl/fl}$;*P0-cre* mice are similar to those of Liu's *Cdc42*$^{fl/fl}$;*Wnt1-cre* mice, though the bilateral cleft lip seen in Liu's *Cdc42*$^{fl/fl}$;*Wnt1-cre* mice were not found in the present mice. In their study, Liu et al. (2013) used TUNEL and phosphorylated histone H3 staining assays to show that inactivation of Cdc42 did not significantly affect CNC-derived cell survival or proliferation in pharyngeal arches. We also investigated the expression of *CyclinD*$_1$ in palates of *Cdc42*$^{fl/fl}$;*P0-cre* mice obtained on E12.5, E13.5, and E14.5 to examine the effects of cell cycle progression on proliferation of palatal cells, and found no differences between the *Cdc42*$^{fl/fl}$;*P0-cre* and control mice (Suppl. Fig. 1). Furthermore, Liu et al. (2013) suggested that Cdc42 is an important effector in Bmp2-induced NCC cytoskeleton remodeling and migration through p38 MAPK activation, a potential downstream effector of Cdc42. However, the role of Cdc42 in NCC cytoskeleton remodeling and migration is controversial (Fuchs et al., 2009), and additional studies are needed to determine the mechanisms of palatal development related to Cdc42 function.

A previous review noted that palatal shelf defects that result in cleft palate during palatogenesis can be classified into 5 categories; failure of palatal shelf formation, fusion with tongue or mandible, failure of palatal shelf elevation, failure of shelves to meet following elevation, and persistence of medial edge epithelium (Chai and Maxson, 2006). We found that the morphological structures of palatal shelves in *Cdc42*$^{fl/fl}$;*P0-cre* mice were comparable with those of *Cdc42*$^{fl/fl}$ mice up to E14.5 (Fig. 3B, F), while a pronounced aberration in palate development was observed in the *Cdc42*$^{fl/fl}$;*P0-cre* mice after E15.5, by which time the palate shelves elevate and meet (Fig. 3C, G). The general consensus is that palatal shelf elevation is a rapid movement triggered by both intrinsic forces within the palatal shelf proper, including cell-proliferation ability in the palatal shelf, and influences from other craniofacial and oral structures, including movement of the tongue and mandible growth (Gritli-Linde, 2007). A variety of genes are involved in the process of palate shelf elevation and further studies of elevation failure are necessary. It is interesting that previous studies have found that palatal shelves remained separated from each other in *Cdc42*$^{fl/fl}$;*P0-cre* mice (Bi et al., 2001; Ito et al., 2003; Dudas et al., 2004; Xu et al., 2005).

In conclusion, our results demonstrate that Cdc42 plays a crucial role in facial and palatal formation during craniofacial development. Though our study has a limitation that deletion of Cdc42 gene in the palates is mosaic, they provide important information for clinical studies to identify patients with cleft palate as well as families with a high risk of cleft palate related to cellular signaling of Rho-family proteins. Moreover, these findings are considered useful for prevention of cleft palate and development of non-surgical correction strategies.

Supplementary data to this article can be found online at http://dx.doi.org/10.1016/j.bonr.2016.01.001.

Acknowledgments

We would like to thank Mr. Ryo Nagahama, Mr. Katsuhiro Hiranuma, and Ms. Mikiko Ikehata for their help with our study. This work was supported in part by the Project to Establish Strategic Research Center for Innovative Dentistry by the Ministry of Education, Culture, Sports, Science and Technology of Japan, and Grants-in-Aid for Scientific Research from the Japan Society for the Promotion of Science (AY: 15K11051).

References

Aizawa, R., Yamada, A., Suzuki, D., Iimura, T., Kassai, H., Harada, T., Tsukasaki, M., Yamamoto, G., Tachikawa, T., Nakao, K., Yamamoto, M., Yamaguchi, A., Aiba, A., Kamijo, R., 2012. Cdc42 is required for chondrogenesis and interdigital programmed cell death during limb development. Mech. Dev. 129, 38–50.

Bi, W., Huang, W., Whitworth, D.J., Deng, J.M., Zhang, Z., Behringer, R.R., de Crombrugghe, B., 2001. Haploinsufficiency of Sox9 results in defective cartilage primordia and premature skeletal mineralization. Proc. Natl. Acad. Sci. U. S. A. 98, 6698–6703.

Bishop, A.L., Hall, A., 2000. Rho GTPases and their effector proteins. Biochem. J. 348, 241–255.

Bronner-Fraser, M., 1993. Neural crest cell migration in the developing embryo. Trends Cell Biol. 3, 392–397.

Bronner-Fraser, M., Fraser, S.E., 1988. Cell lineage analysis reveals multipotency of some avian neural crest cells. Nature 335, 161–164.

Chai, Y., Maxson, R.E., 2006. Recent advances in craniofacial morphogenesis. Dev. Dyn. 235, 2353–2375.

Chai, Y., Jiang, X., Ito, Y., Bringas, P., Han, J., Rowitch, D.H., Soriano, P., McMahon, A.P., Sucov, H.M., 2000. Fate of the mammalian cranial neural crest during tooth and mandibular morphogenesis. Development 127, 1671–1679.

Chen, F., Ma, L., Parrini, M.C., Mao, X., Lopez, M., Wu, C., Marks, P.W., Davidson, L., Kwiatkowski, D.J., Kirchhausen, T., Orkin, S.H., Rosen, F.S., Mayer, B.J., Kirschner, M.W., Alt, F.W., 2000. Cdc42 is required for PIP(2)-induced actin polymerization and early development but not for cell viability. Curr. Biol. 10, 758–765.

Cobourne, M.T., 2004. The complex genetics of cleft lip and palate. Eur. J. Orthod. 26, 7–16.

Dudas, M., Sridurongrit, S., Nagy, A., Okazaki, K., Kaartinen, V., 2004. Craniofacial defects in mice lacking BMP type I receptor Alk2 in neural crest cells. Mech. Dev. 121, 173–182.

Etienne-Manneville, S., Hall, A., 2002. Rho GTPases in cell biology. Nature 420, 629–635.

Ferguson, M.W., 1977. The mechanism of palatal shelf elevation and the pathogenesis of cleft palate. Virchows Arch. A Pathol. Anat. Histol. 375, 97–113.

Fuchs, S., Herzog, D., Sumara, G., Buchmann-Moller, S., Civenni, G., Wu, X., Chrostek-Grashoff, A., Suter, U., Ricci, R., Relvas, J.B., Brakebusch, C., Sommer, L., 2009. Stage-specific control of neural crest stem cell proliferation by the small rho GTPases Cdc42 and Rac1. Cell Stem Cell 4, 236–247.

Gritli-Linde, A., 2007. Molecular control of secondary palate development. Dev. Biol. 301, 309–326.

Hall, A., Nobes, C.D., 2000. Rho GTPases: molecular switches that control the organization and dynamics of the actin cytoskeleton. Philos. Trans. R. Soc. Lond. Ser. B Biol. Sci. 355, 965–970.

Ito, Y., Yeo, J.Y., Chytil, A., Han, J., Bringas, P., Nakajima, A., Shuler, C.F., Moses, H.L., Chai, Y., 2003. Conditional inactivation of Tgfbr2 in cranial neural crest causes cleft palate and calvaria defects. Development 130, 5269–5280.

Jaffe, A.B., Hall, A., 2005. Rho GTPases: biochemistry and biology. Annu. Rev. Cell Dev. Biol. 21, 247–269.

Kawamoto, S., Niwa, H., Tashiro, F., Sano, S., Kondoh, G., Takeda, J., Tabayashi, K., Miyazaki, J., 2000. A novel reporter mouse strain that expresses enhanced green fluorescent protein upon Cre-mediated recombination. FEBS Lett. 470, 263–268.

Le Douarin, N.M., Creuzet, S., Couly, G., Dupin, E., 2004. Neural crest cell plasticity and its limits. Development 131, 4637–4650.

Levi, B., Brugman, S., Wong, V.W., Grova, M., Longaker, M.T., Wan, D.C., 2011. Palatogenesis: engineering, pathways and pathologies. Organogenesis 7, 242–254.

Liu, K.J., Arron, J.R., Stankunas, K., Crabtree, G.R., Longaker, M.T., 2007. Chemical rescue of cleft palate and midline defects in conditional GSK-3beta mice. Nature 446, 79–82.

Liu, Y., Jin, Y., Li, J., Seto, E., Kuo, E., Yu, W., Schwartz, R.J., Blazo, M., Zhang, S.L., Peng, X., 2013. Inactivation of Cdc42 in neural crest cells causes craniofacial and cardiovascular morphogenesis defects. Dev. Biol. 383, 239–252.

Schutte, B.C., Murray, J.C., 1999. The many faces and factors of orofacial clefts. Hum. Mol. Genet. 8, 1853–1859.

Selleck, M.A., Scherson, T.Y., Bronner-Fraser, M., 1993. Origins of neural crest cell diversity. Dev. Biol. 159, 1–11.

Shah, N.M., Groves, A.K., Anderson, D.J., 1996. Alternative neural crest cell fates are instructively promoted by TGFbeta superfamily members. Cell 85, 331–343.

Soriano, P., 1999. Generalized lacZ expression with the ROSA26 Cre reporter strain. Nat. Genet. 21, 70–71.

Suzuki, D., Yamada, A., Amano, T., Yasuhara, R., Kimura, A., Sakahara, M., Tsumaki, N., Takeda, S., Tamura, M., Nakamura, M., Wada, N., Nohno, T., Shiroishi, T., Aiba, A., Kamijo, R., 2009. Essential mesenchymal role of small GTPase Rac1 in interdigital programmed cell death during limb development. Dev. Biol. 335, 396–406.

Van Aelst, L., D'Souza-Schorey, C., 1997. Rho GTPases and signaling networks. Genes Dev. 11, 2295–2322.

Vanderas, A.P., 1987. Incidence of cleft lip, cleft palate, and cleft lip and palate among races: a review. Cleft Palate J. 24, 216–225.

Wilkie, A.O., Morriss-Kay, G.M., 2001. Genetics of craniofacial development and malformation. Nat. Rev. Genet. 2, 458–468.

Xu, X., Bringas, P., Soriano, P., Chai, Y., 2005. PDGFR-alpha signaling is critical for tooth cusp and palate morphogenesis. Dev. Dyn. 232, 75–84.

Yamauchi, Y., Abe, K., Mantani, A., Hitoshi, Y., Suzuki, M., Osuzu, F., Kuratani, S., Yamamura, K., 1999. A novel transgenic technique that allows specific marking of the neural crest cell lineage in mice. Dev. Biol. 212, 191–203.